

# Hydrogen production from dimethyl ether steam reforming over composite catalysts of copper ferrite spinel and alumina

Kajornsak Faungnawakij<sup>a,b</sup>, Yohei Tanaka<sup>b</sup>, Naohiro Shimoda<sup>b</sup>,  
Tetsuya Fukunaga<sup>c</sup>, Ryuji Kikuchi<sup>b</sup>, Koichi Eguchi<sup>b,\*</sup>

<sup>a</sup>Japan Science and Technology Agency (JST), Innovation Plaza Kyoto, 1-30 Goryo-Ohara Nishikyo-ku, Kyoto 615-8245, Japan

<sup>b</sup>Department of Energy and Hydrocarbon Chemistry, Graduate School of Engineering, Kyoto University, Nishikyo-ku, Kyoto 615-8510, Japan

<sup>c</sup>Central Research Laboratories, Idemitsu Kosan Co., Ltd., 1280 Kami-izumi, Sodegaura, Chiba 299-0293, Japan

Received 27 June 2006; received in revised form 18 December 2006; accepted 13 February 2007

Available online 16 February 2007

## Abstract

Dimethyl ether steam reforming (DME SR) was performed over composite catalysts of copper ferrite spinel ( $\text{CuFe}_2\text{O}_4$ ) and alumina for hydrogen production, applicable to fuel cell. A highly active composite was achieved when the calcination temperature of the Cu spinel was at  $900^\circ\text{C}$  and that of the alumina was at or below  $700^\circ\text{C}$ . The calcination temperature strongly affected the crystallinity and reducibility of the copper ferrite spinel and the acidity of alumina. The composite catalysts both with and without pre-reduction were active for DME SR when the pre-reduced catalyst exhibited higher initial activity, but longer activation process was observed for the composite catalyst without pre-reduction. DME conversion and hydrogen production significantly depended on gas hourly space velocity (GHSV) and reforming temperatures ( $T_r$ ). DME conversion ( $>95\%$ ),  $\text{H}_2$  production rate ( $\sim 50 \text{ mol kg}_{\text{cat}}^{-1} \text{ h}^{-1}$ ), and  $\text{H}_2$  concentration (ca. 73%) were achieved at  $T_r$  of  $350^\circ\text{C}$  and GHSV of  $1500 \text{ h}^{-1}$ . The maximum  $\text{H}_2$  production rate of  $120 \text{ mol kg}_{\text{cat}}^{-1} \text{ h}^{-1}$  was found at  $T_r$  of  $450^\circ\text{C}$  and GHSV of  $4000 \text{ h}^{-1}$ . Mixing state of the copper spinel and the alumina was also investigated. After mixing with alumina, the present  $\text{CuFe}_2\text{O}_4$  markedly exhibited excellent activity for DME SR in comparison to the commercial  $\text{CuFe}_2\text{O}_4$  and  $\text{Cu/ZnO/Al}_2\text{O}_3$ .

© 2007 Elsevier B.V. All rights reserved.

**Keywords:** Copper ferrite spinel; Steam reforming; Dimethyl ether; Hydrogen; Fuel cell

## 1. Introduction

Development of hydrogen-generating process has been urged worldwide. Hydrogen fuel is regarded as a clean energy for future. The use of hydrogen as fuel for fuel cell applications has been recognized as an efficient technology for electricity generation. In recent years, some processes, e.g., reforming of fuels [1–18] and water splitting [19,20], have attracted much attention as an attractive technology for production of hydrogen. As for the reforming process, methanol [1–4], ethanol [5–8], natural gas [9–12], and dimethyl ether [13–18], have been used as fuels for hydrogen production. Steam reforming (SR), partial oxidation (PO), and autothermal reforming (ATR) are the major processes for reforming of

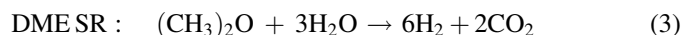
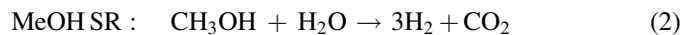
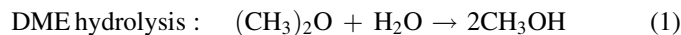
those fuels. PO and ATR processes provide an advantage of fast start-up time due to exothermic nature of oxidation reactions. However, the PO and ATR give a lower reformat quality than the SR, i.e., lower hydrogen production yield, higher rate of side reactions, and by-products. Thermodynamic study of such reforming processes has been carried out to evaluate the equilibrium composition [21,22].

Recently, dimethyl ether (DME) has become a promising candidate as hydrogen source to be used in fuel-processors. DME has a high hydrogen-to-carbon ratio and a high energy density, and is non-corrosive and non-toxic. DME can be easily handled, stored, and transported. In addition, the infrastructure of LPG can readily be adapted for DME due to their similar physical properties. Production of hydrogen from DME SR process has been presently developed [14–18]. DME has no C–C bond; therefore it can be reformed at relatively low temperature ( $200\text{--}450^\circ\text{C}$ ). Steam reforming of DME comprises two reactions in sequence: DME hydrolysis and

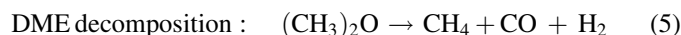
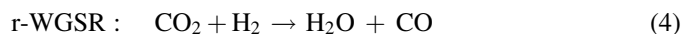
\* Corresponding author. Tel.: +81 75 383 2519; fax: +81 75 383 2520.

E-mail address: [eguchi@scl.kyoto-u.ac.jp](mailto:eguchi@scl.kyoto-u.ac.jp) (K. Eguchi).

methanol (MeOH) steam reforming, as expressed in Eqs. (1) and (2), respectively.



DME hydrolysis actively takes place over acidic site of acid catalysts such as alumina and zeolite, while MeOH SR proceeds over metal catalysts, Cu- and Pt-based catalysts. Besides DME SR, reverse water gas shift reaction (r-WGSR) generally takes place over such metal catalysts during the reforming process. In addition, methane would be generated via DME decomposition in the case that strong acidic catalyst or high reforming temperatures are employed.



We have reported that the composite catalysts of Cu-based spinel oxide-type and alumina or zeolite are highly active for DME SR [16,18]. In this work, the preparation condition of the Cu-based spinel and that of alumina along with a mixing state of the composite catalyst were investigated to fine tune the optimal condition. Influence of gas hourly space velocity (GHSV) was also studied.

## 2. Experimental

### 2.1. Catalyst preparation

Copper ferrite spinel,  $\text{CuFe}_2\text{O}_4$  was prepared by a citric acid complex method. The method can effectively accommodate different cations in the complex, resulting in uniform mixing of the cations [23]. An aqueous solution of copper and iron nitrates ( $\text{Cu}(\text{NO}_3)_2 \cdot 3\text{H}_2\text{O}$  and  $\text{Fe}(\text{NO}_3)_3 \cdot 9\text{H}_2\text{O}$ ) was stirred at 60 °C for 2 h, followed by addition of citric acid. The solution was continued to be kept at 60 °C for 1 h to make it homogeneous. The solution was then heated up to 90 °C to evaporate water. The precipitate obtained was heated up to 140–200 °C until oxide powders were achieved. The powder was calcined in air at 500, 700, 900 or 1100 °C for 10 h. Alumina, ALO8 provided by the Catalysis Society of Japan was calcined in air at 500, 700, 900 or 1100 °C for 0.5 h prior to investigation. The Cu spinel was physically mixed with the alumina catalyst at a fixed weight ratio of 2:1. The composite catalyst was pelletized in the range of 0.85–1.7 mm, unless otherwise stated.

### 2.2. Catalyst characterization

Temperature programmed reduction (TPR) was conducted using CHEMBET-3000. The catalyst sample (25 mg) was reduced in 5%  $\text{H}_2$  in Ar at a flow rate of 30 ml/min (25 °C, 1 atm) with an increasing rate of temperature of 10 K/min. Ammonia-

temperature programmed desorption ( $\text{NH}_3$ -TPD) was used for measurement of acidity of catalysts. Specific surface area of catalysts after degassing at 300 °C for 0.5 h was determined by the conventional BET method with  $\text{N}_2$  adsorption using a Shimadzu Gemini 2375 instrument. Powder X-ray diffraction (XRD) patterns were obtained using Rigaku RINT1400 equipped with Cu  $\text{K}\alpha$  radiation source. The crystallite sizes were calculated from the full width at half maximum of  $\text{CuFe}_2\text{O}_4$  ( $2\theta \approx 36^\circ$ ) and Cu ( $2\theta \approx 43^\circ$ ) peaks using Scherrer equation. Relative crystallinity of spinel was defined as  $C_i (\%) = 100P_i/P_m$ , where  $P_i$  is an intensity of a diffraction peak at  $2\theta \approx 36^\circ$  and  $P_m$  is the maximum  $P_i$  observed for the sample calcined at 900 °C.

### 2.3. Evaluation of catalytic activity

The evaluation of catalytic activity was carried out using a conventional flow reactor under atmospheric pressure. Prior to the evaluation of catalysts, reduction of the catalyst was carried out at 350 °C for 3 h in 10%  $\text{H}_2/\text{N}_2$ . DME and steam at a fixed steam-to-carbon ratio ( $S/C = 2.5$ ) were supplied to a pre-heater at temperature ca. 150 °C, and then to the catalyst bed at designed reaction temperatures through mass flow controllers. The reaction temperature was varied in the range of 250–450 °C.

Compositions of influent and effluent gas were analyzed by on-line gas chromatographs equipped with FID (Shimadzu, GC-9A) and TCD (VARIAN, CP-4900). The steam in the feed and reformat was trapped by a condenser at ca. 3 °C before the gas analysis. A Poraplot U column was used for separation of DME, methanol, and  $\text{CO}_2$ , and a molecular sieve 5A column was used for separation of  $\text{H}_2$ ,  $\text{N}_2$ ,  $\text{CH}_4$ , and CO. Selectivity to CO and  $\text{CH}_4$  was defined as follows:

$$\text{CH}_4 \text{ selectivity } (\%) = \frac{F_{\text{CH}_4}}{F_{\text{CH}_4} + F_{\text{CO}} + F_{\text{CO}_2}} \times 100 \quad (6)$$

$$\text{CO selectivity } (\%) = \frac{F_{\text{CO}}}{F_{\text{CH}_4} + F_{\text{CO}} + F_{\text{CO}_2}} \times 100 \quad (7)$$

where  $F_{\text{CH}_4}$ ,  $F_{\text{CO}}$  and  $F_{\text{CO}_2}$  are the effluent molar flow rates of  $\text{CH}_4$ , CO, and  $\text{CO}_2$ , respectively.

## 3. Results and discussion

### 3.1. Effect of calcination temperature of $\text{CuFe}_2\text{O}_4$

The Cu-based spinel oxide mixed with alumina is highly active for DME SR [16,18]. We have used the copper ferrite spinel mixed with various types of acidic catalyst to evaluate the role of the acidic catalysts [18]. It is expected that the difference in calcination temperature affects the crystallinity, reducibility and surface area, resulting in a change of catalytic activity. In the present work, the copper ferrite spinel oxide was calcined at 500, 700, 900, and 1100 °C, hereafter denoted as Cu–Fe500, Cu–Fe700, Cu–Fe900, and Cu–Fe1100, respectively.

Fig. 1 shows the XRD patterns of  $\text{CuFe}_2\text{O}_4$  calcined at varied temperatures along with the as-prepared sample, and Table 1 shows their BET surface area, crystalline phase, crystallite size, and relative crystallinity of spinel. Copper iron spinel

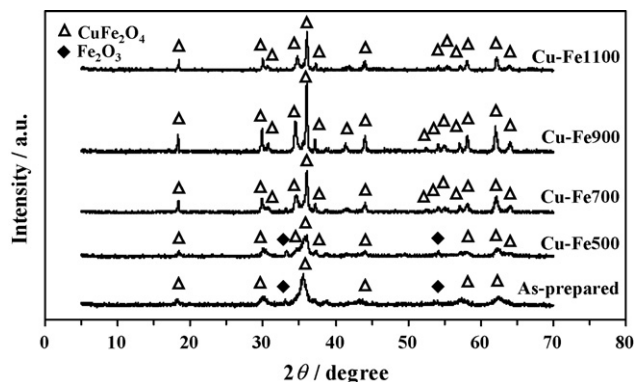


Fig. 1. XRD patterns of  $\text{CuFe}_2\text{O}_4$  as-prepared, and calcined at 500, 700, 900, and 1100 °C.

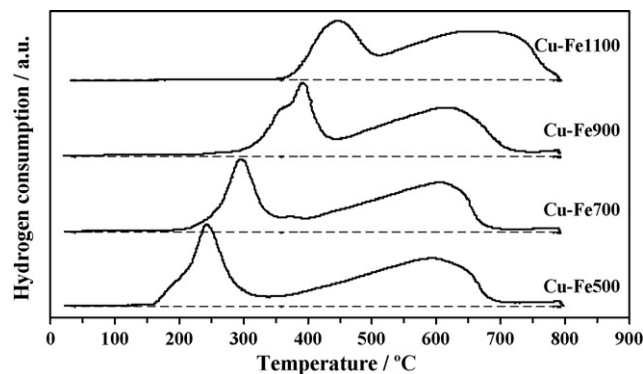


Fig. 2. TPR patterns of  $\text{CuFe}_2\text{O}_4$  calcined at 500, 700, 900, and 1100 °C. TPR conditions: 10 K/min in 5%  $\text{H}_2/\text{Ar}$ .

as-prepared comprises mainly a  $\text{CuFe}_2\text{O}_4$  phase and partly  $\text{Fe}_2\text{O}_3$  phase. The crystallinity of the catalyst scarcely increased when it was calcined at 500 °C, and significantly increased when it was calcined at or above 700 °C. Cu–Fe700, Cu–Fe900, and Cu–Fe1100 have a single crystalline phase of copper ferrite spinel. The crystallite size was minimum at 9 nm for Cu–Fe500 and was maximum at 54 nm for Cu–Fe900. The degree of crystallization and crystallite size of  $\text{CuFe}_2\text{O}_4$  increased up to 900 °C, and then inversely decreased at 1100 °C. Spinel with lower crystallinity gives rise to wider diffraction lines with lower intensity. The change of crystallinity indicated that the stoichiometric  $\text{CuFe}_2\text{O}_4$  crystal grew with an increase in calcination temperature up to 900 °C, and the  $\text{CuFe}_2\text{O}_4$  phase remained stable in the temperature range of 500–900 °C. The crystal growth and a loss of porosity lessened BET surface area from 6.0 (Cu–Fe500) to 0.5  $\text{m}^2/\text{g}$  (Cu–Fe1100). Tanaka et al. [24] reported that BET surface area of the Cu–Mn spinel oxide decreased with an increase in calcination temperature because of a shrinkage of catalyst particles.

Fig. 2 shows TPR profiles of the  $\text{CuFe}_2\text{O}_4$  calcined at varied temperatures. All profiles consisted of two major peaks. The first peak appearing at lower temperature was ascribed to the reduction of  $\text{CuFe}_2\text{O}_4$  to metallic Cu and  $\text{Fe}_2\text{O}_3$ . Instantly, the  $\text{Fe}_2\text{O}_3$  continued to be reduced to  $\text{Fe}_3\text{O}_4$ . The second peak was ascribed to the reduction of  $\text{Fe}_3\text{O}_4$  to Fe via FeO. The first peak shifted to the higher reduction temperature when the calcination temperature increased up to 1100 °C. Consequently, the second peak also shifted to the right on the profile. This suggested that the catalyst calcined at lower temperature contains more reducible species.

Fig. 3 displays the DME SR activity in terms of DME conversion and hydrogen production of the calcined Cu spinel mixed with alumina (Cu–Fe500 + ALO700, Cu–Fe700 +

ALO700, and Cu–Fe900 + ALO700) as a function of reforming temperature. The catalytic activity increased with an increase in calcination temperature from 500 to 900 °C. Cu–Fe900 showed the best performance in the temperature range studied. According to XRD analysis as shown in Fig. 4, the reacted catalysts consisted of two crystalline phases of metallic Cu and  $\text{Fe}_3\text{O}_4$ . Crystallite size of Cu in the reacted catalysts decreased with an increase in calcination temperatures (Cu–Fe500 = ~200 nm, Cu–Fe700 = 69 nm, Cu–Fe900 = 54 nm). The size of Cu after reduction and reaction for Cu–Fe900 was 54 and 50 nm, respectively. This indicated that the copper ferrite spinel calcined at 900 °C could suppress Cu-sintering even at high reaction temperatures of 350–450 °C, where Cu-sintering can proceed severely over conventional Cu-based catalysts.

The composite catalysts with and without pre-reduction were investigated for DME SR activity. DME conversion and hydrogen production from the catalysts with and without pre-reduction were depicted in Fig. 5. As a result, both reduced and un-reduced catalysts were active for DME SR. The reduced catalyst provided higher DME conversion and hydrogen production rate than the un-reduced one. However, the difference in activity became smaller when the temperature increased up to 400–450 °C. According to XRD analysis, the crystalline phase of the un-reduced catalyst comprised two phases of metallic copper and  $\text{Fe}_3\text{O}_4$  after DME SR reaction. Therefore, the catalyst without pre-reduction could be instantly reduced by the hydrogen produced from DME SR. According to the TPR profile of Cu–Fe900, the reduction of the spinel started from ca. 230 °C and then the spinel was rapidly reduced from the temperatures above 300 °C. The two catalysts are expected to show a comparable activity since copper species of both catalysts were reduced and activated under the reducing condition of DME SR after sufficient-time operation. Prolonged

Table 1  
BET surface area, crystalline phase, crystallite size, and relative crystallinity of copper iron spinels calcined at various temperatures

Catalyst	BET surface area ( $\text{m}^2/\text{g}$ )	Crystalline phase	Crystallite size (nm)	Relative crystallinity of spinel (%)
Cu–Fe500	6.0	$\text{CuFe}_2\text{O}_4$ , $\text{Fe}_2\text{O}_3$	9	34
Cu–Fe700	3.5	$\text{CuFe}_2\text{O}_4$	28	60
Cu–Fe900	1.0	$\text{CuFe}_2\text{O}_4$	54	100 (reference)
Cu–Fe1100	0.5	$\text{CuFe}_2\text{O}_4$	50	57

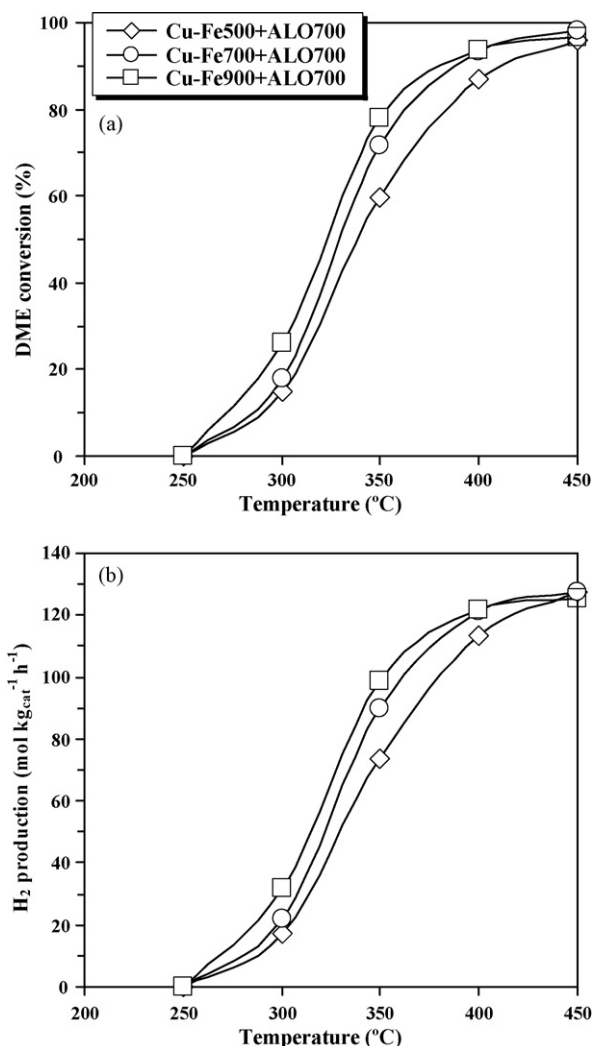


Fig. 3. Effect of calcination temperature of copper ferrite spinel on (a) DME conversion and (b) hydrogen production from DME SR over  $\text{CuFe}_2\text{O}_4 + \text{ALO700}$ . Reduction conditions: 350 °C, 3 h in 10%  $\text{H}_2/\text{N}_2$ . Reaction conditions:  $\text{S/C} = 2.5$ ;  $\text{DME} = 16.7\%$ ; steam = 83.3%;  $\text{GHSV} = 4000 \text{ h}^{-1}$ .

exposure of the unreduced catalyst to the reaction atmosphere appears to be effective in reducing the spinel.

### 3.2. Effect of calcination temperature of $\text{Al}_2\text{O}_3$

The alumina, as a weakly acidic catalyst, was known to be an active catalyst for DME hydrolysis. Transformation of alumina phase relates with calcination temperature, and should impact its catalytic activity. Gamma phase derived from boehmite was formed at 450–750 °C. Delta, theta, and alpha phases were consecutively formed when the temperatures increased to 750, 950, and 1050 °C, respectively [25]. Here, we investigated the effect of alumina phase by varying the calcination temperature from 500 to 1100 °C. Table 2 shows BET surface area, pore volume, acid amount, and alumina phase of the alumina as-obtained and calcined at 500, 700, 900, or 1100 °C, denoted as ALO–, ALO500, ALO700, ALO900, and ALO1100, respectively. BET surface of the alumina obviously decreased with increase in calcination temperature because of its crystal

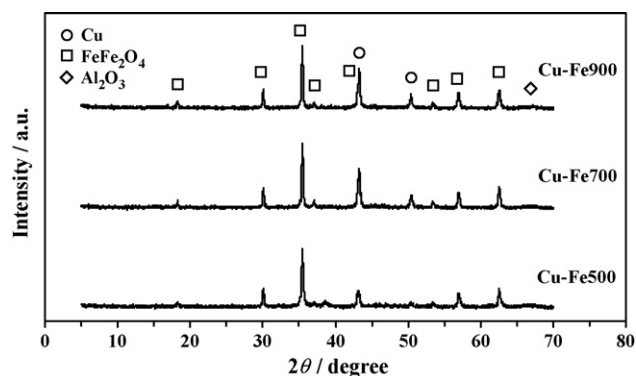


Fig. 4. XRD patterns of  $\text{CuFe}_2\text{O}_4$  calcined at 500, 700, and 900 °C after SR reaction.

growth. Pore volume was slightly decreased from 1.2 to 1.1  $\text{cm}^3/\text{g}$ . Acid amount of the alumina also decreased from 50 to ca. 5  $\mu\text{mol}/\text{g}$  when the calcination temperature was raised up from 500 to 1100 °C.

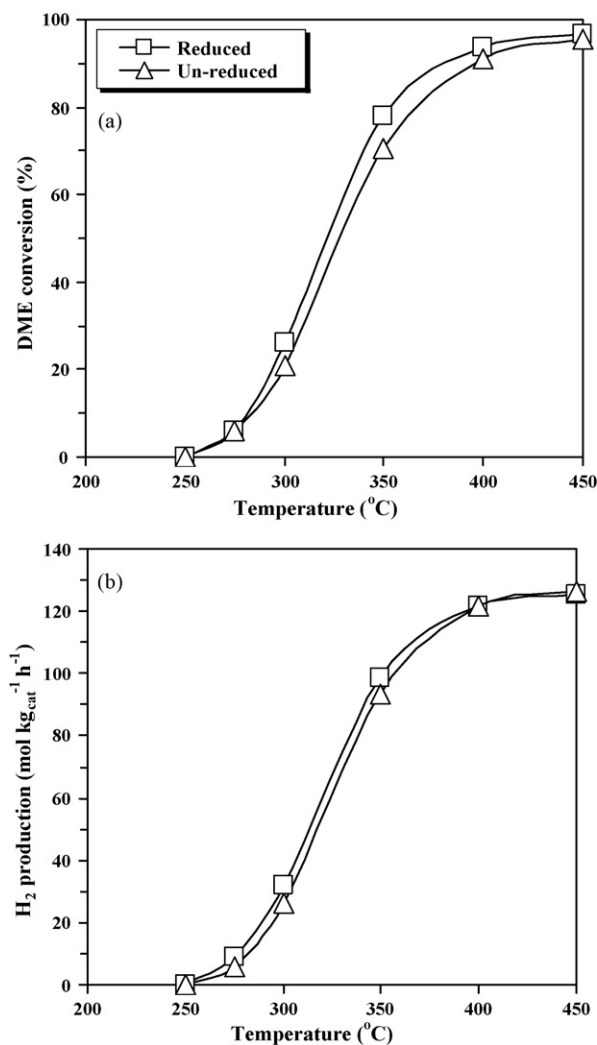


Fig. 5. Effect of reduction treatment of  $\text{Cu-Fe900} + \text{ALO700}$  on (a) DME conversion and (b) hydrogen production from DME SR. Reduction conditions: 350 °C, 3 h in 10%  $\text{H}_2/\text{N}_2$ . Reaction conditions:  $\text{S/C} = 2.5$ ;  $\text{DME} = 16.7\%$ ; steam = 83.3%;  $\text{GHSV} = 4000 \text{ h}^{-1}$ .

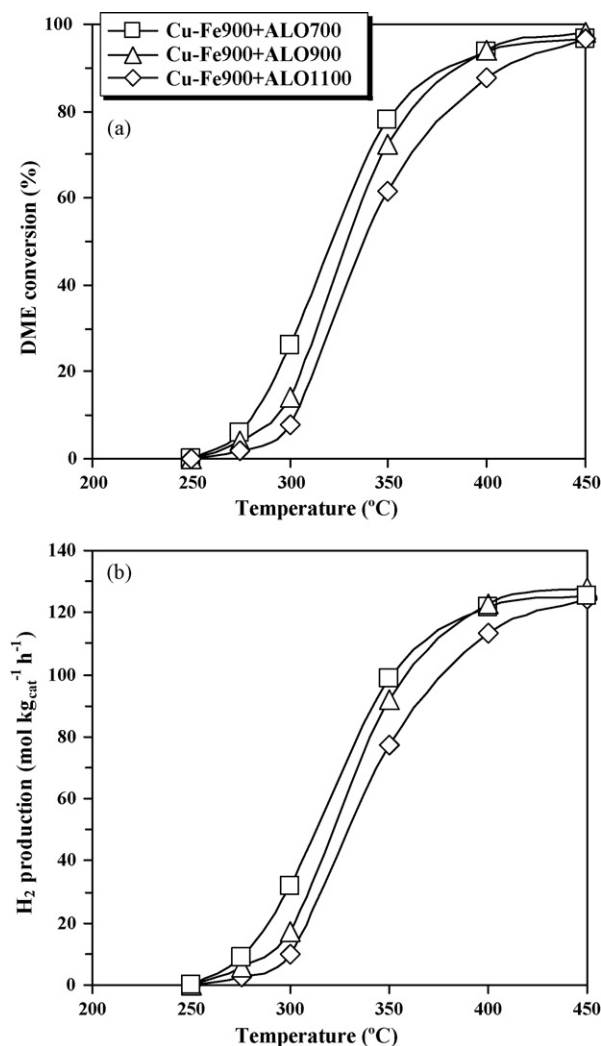


Fig. 6. Effect of calcination temperature of alumina on (a) DME conversion and (b) hydrogen production from DME SR over Cu–Fe900 + ALO8. Reduction conditions: 350 °C, 3 h in 10% H<sub>2</sub>/N<sub>2</sub>. Reaction conditions: S/C = 2.5; DME = 16.7%, steam = 83.3%; GHSV = 4000 h<sup>-1</sup>.

The DME SR activity of the Cu–Fe900 mixed with alumina (Cu–Fe900 + ALO700, Cu–Fe900 + ALO900, and Cu–Fe900 + ALO1100) was illustrated as a function of reforming temperature in Fig. 6. The catalytic activity of Cu–Fe900 + ALO700 was significantly higher than that of Cu–Fe900 + ALO900 and Cu–Fe900 + ALO1100. This result indicated that gamma alumina was highly active for DME SR, whereas delta and alpha alumina exhibited low DME hydrolysis activity. From NH<sub>3</sub>-TPD analysis, the acid amount

of alumina decreased with an increase in calcination temperature from 700 to 1100 °C. This should be ascribed to the loss of an active surface area and a change of surface properties, resulting in the drop of DME SR activity. Note that the catalytic activities of Cu–Fe900 + ALO–, Cu–Fe900 + ALO500 and Cu–Fe900 + ALO700 were nearly comparable although the results were not shown here.

### 3.3. Effect of mixing state of CuFe<sub>2</sub>O<sub>4</sub> and Al<sub>2</sub>O<sub>3</sub>

At the moment, two types of catalysts, namely, Cu catalyst and acidic catalyst are generally needed for DME SR. A mixing state of the two catalysts should play an important role in the catalytic activity. In this study, a mechanical mixing of the Cu spinel and alumina was used for preparation of the composite catalyst. Here, the three mixing states, i.e., separated, granule-mixed and powder-milled-mixed, of copper ferrite (Cu–Fe900) and alumina (ALO700) were investigated. In the case of separated, the spinel catalyst and the alumina were separately pelletized and then randomly placed in the catalyst bed. The granule-mixed catalyst represented the mechanical mixing of the spinel and the alumina without milling in an alumina mortar prior to pelletization, while the powder-milled-mixed catalyst was prepared by milling the two catalysts until well-mixed and uniform composite catalyst was achieved (ca. 1 h mixing time). The catalytic activity is shown as a function of temperature in Fig. 7. The mixed catalysts exhibited obviously higher catalytic activity than the separated one. DME hydrolysis over alumina rapidly followed by MeOH SR over Cu catalyst is expected to contribute to the overall DME SR activity. However, the granule-mixed and the powder-milled-mixed catalysts showed almost same activity, except above 350 °C under the condition studied. It was considered that the mixing state of the granule-mixed catalyst was enhanced during the pelletization by pressing at high pressure.

### 3.4. Effect of GHSV

Fig. 8 shows the effect of gas hourly space velocity (GHSV) on a catalytic reforming activity over CuFe<sub>2</sub>O<sub>4</sub> + ALO8. GHSV was varied from 1500–4000 h<sup>-1</sup> by varying the amount of catalyst used for reaction at a constant reaction temperature of 350 °C in this evaluation. The DME conversion increased with decreasing GHSV, corresponding to an increase in flow rate of hydrogen produced. However, hydrogen production rate was observed in a deposit tendency since the amount of catalyst used was intentionally increased to control GHSV. The DME

Table 2  
BET surface area, pore volume, acid amount, and crystalline phase of alumina calcined at various temperatures

Catalyst	BET surface area (m <sup>2</sup> /g)	Pore volume (cm <sup>3</sup> /g)	Acid amount (μmol/g)	Crystalline phase
ALO–	157	1.2	50	Gamma
ALO500	141	1.2	50	Gamma
ALO700	137	1.1	50	Gamma
ALO900	128	1.1	20	Delta
ALO1100	104	1.1	~5	Alpha

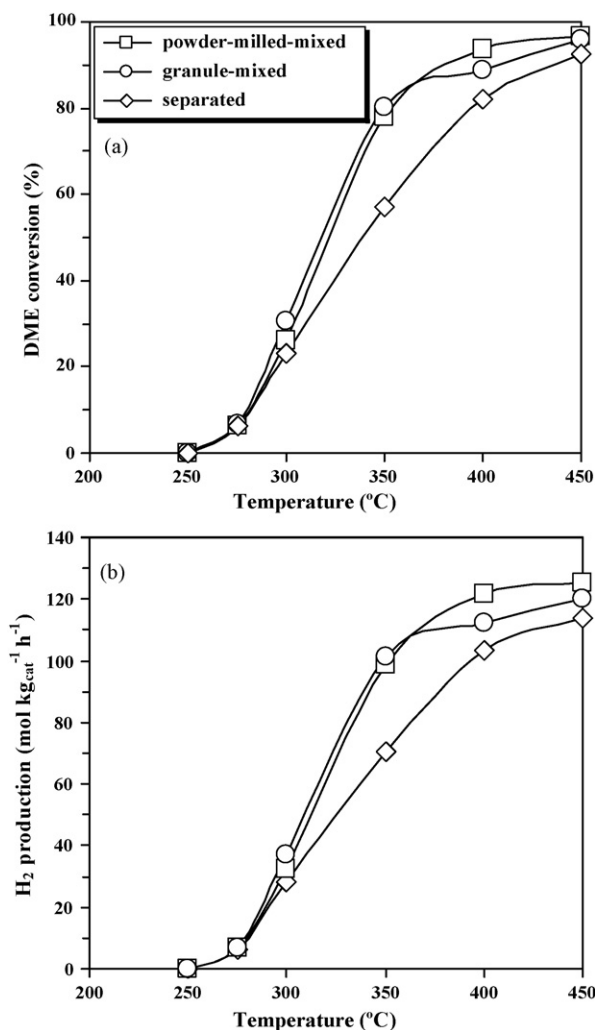


Fig. 7. Effect of mixing state of copper ferrite spinel and alumina on (a) DME conversion and (b) hydrogen production from DME SR. Reduction conditions: 350 °C, 3 h in 10% H<sub>2</sub>/N<sub>2</sub>. Reaction conditions: S/C = 2.5; DME = 16.7%, steam = 83.3%; GHSV = 4000 h<sup>-1</sup>.

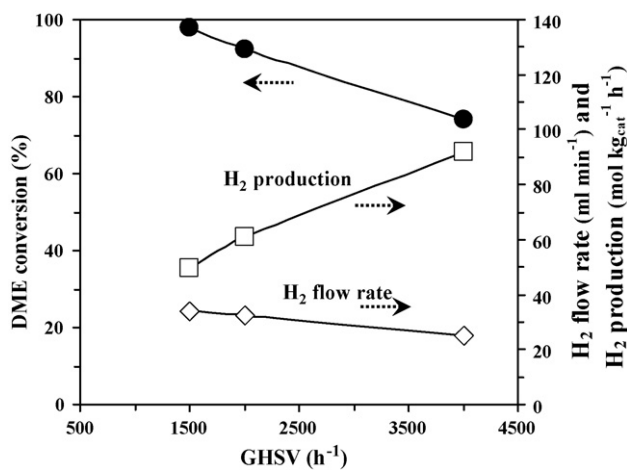


Fig. 8. Effect of GHSV on catalytic reforming activity of Cu-Fe900 + ALO700. Reduction conditions: 350 °C, 3 h in 10% H<sub>2</sub>/N<sub>2</sub>. Reaction conditions: S/C = 2.5; DME = 16.7%, steam = 83.3%.

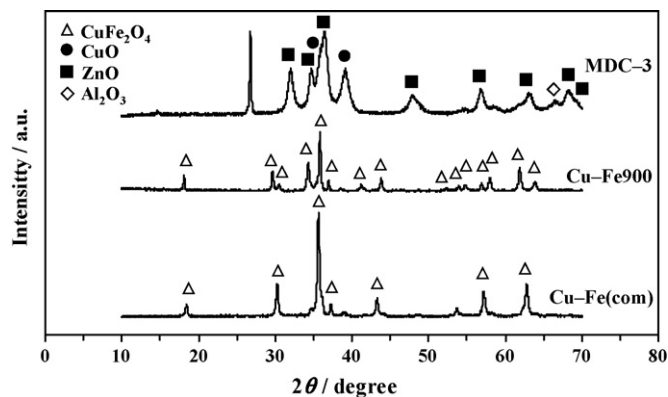


Fig. 9. XRD patterns of MDC-3, Cu-Fe(com), and Cu-Fe900.

conversion increased from ca. 74% to 98% when the GHSV decreased from 4000 to 1500 h<sup>-1</sup>. Meanwhile, hydrogen flow rate and hydrogen production rate were changed from ca. 25 to 34 ml/min, and ca. 90 to 50 mol kg<sub>cat</sub><sup>-1</sup> h<sup>-1</sup>, respectively.

### 3.5. Comparison of the present CuFe<sub>2</sub>O<sub>4</sub>, commercial CuFe<sub>2</sub>O<sub>4</sub>, and commercial Cu/ZnO/Al<sub>2</sub>O<sub>3</sub>

The commercial CuFe<sub>2</sub>O<sub>4</sub> (CuFe<sub>2</sub>O<sub>4</sub> hereafter referred as Cu-Fe(com), 40 nm (XRD), BET = 20 m<sup>2</sup>/g) from Aldrich and the commercial Cu/ZnO/Al<sub>2</sub>O<sub>3</sub> (MDC-3, BET = 72 m<sup>2</sup>/g) from Süd-Chemie were used as a reference for comparison of the DME SR activity. XRD patterns of MDC-3, Cu-Fe(com), and Cu-Fe900 were shown in Fig. 9. The MDC-3 composed of CuO, ZnO, and Al<sub>2</sub>O<sub>3</sub> phases. The CuO phase would be reduced to metallic Cu prior to reaction test. The Cu-Fe(com) and Cu-Fe900 samples comprised pure spinel phase with different crystallinity. BET surface area of Cu-Fe(com) (20 m<sup>2</sup>/g) is much higher than that of Cu-Fe900 (ca. 1 m<sup>2</sup>/g).

Fig. 10 illustrates the DME conversion, hydrogen production, and selectivity to CO and CH<sub>4</sub> over Cu-Fe900 + ALO700, Cu-Fe(com) + ALO700, Cu/ZnO/Al<sub>2</sub>O<sub>3</sub> + ALO700, Cu/ZnO/Al<sub>2</sub>O<sub>3</sub>, and Cu-Fe900. As clearly seen, the Cu-Fe900 + ALO700 exhibited highest DME conversion and hydrogen production throughout the temperature range studies. The Cu-Fe(com) + ALO8 provided higher activity than Cu/ZnO/Al<sub>2</sub>O<sub>3</sub> in the temperatures below 400 °C, but became slightly lower when the temperature increased up to 450 °C. Cu/ZnO/Al<sub>2</sub>O<sub>3</sub> had higher DME SR activity than Cu-Fe spinel alone since DME hydrolysis could take place over the Al<sub>2</sub>O<sub>3</sub>. Selectivity to CH<sub>4</sub> over Cu/ZnO/Al<sub>2</sub>O<sub>3</sub> was drastically higher than that over Cu-Fe900, indicating the higher DME decomposition rate. As a result, selectivity to CO of Cu/ZnO/Al<sub>2</sub>O<sub>3</sub> was lower than that of Cu-Fe900. Concentrations of DME, H<sub>2</sub>, CO<sub>2</sub>, CO, and CH<sub>4</sub> of effluent reformat from DME SR over Cu-Fe900 + ALO700 are plotted as a function of temperature in Fig. 11. The concentrations were analyzed based on a dry basis without dilution of nitrogen in the reformat. The concentration of DME rapidly dropped from ca. 100% to 3% with increasing temperature from 250 to 350 °C. Meantime, the concentration of hydrogen and carbon dioxide rapidly increased from 0% to 24% and 0% to 72%, respectively. Further increase in

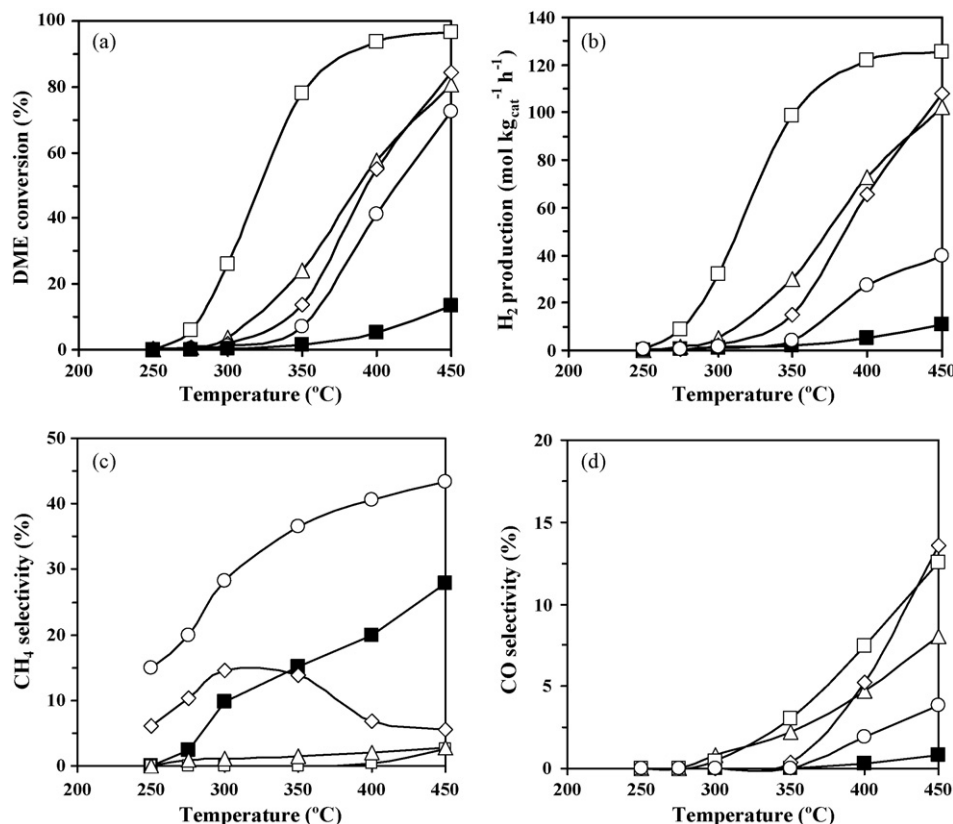


Fig. 10. Comparison of DME SR activity of Cu catalysts on (a) DME conversion, (b) hydrogen production, (c) CH<sub>4</sub> selectivity, and (d) CO selectivity: (□) Cu–Fe900 + ALO700, (△) Cu–Fe(com) + ALO700, (◇) Cu/ZnO/Al<sub>2</sub>O<sub>3</sub> + ALO700, (○) Cu/ZnO/Al<sub>2</sub>O<sub>3</sub>, and (■) Cu–Fe900. Reduction conditions: 350 °C, 3 h in 10% H<sub>2</sub>/N<sub>2</sub>. Reaction conditions: S/C = 2.5; DME = 16.7%, steam = 83.3%; GHSV = 4000 h<sup>-1</sup>.

temperature above 350 °C scarcely decreased concentrations of DME, hydrogen, and carbon dioxide. This is because DME SR accompanying with r-WGSR was accelerated. DME decomposition was negligible over the Cu spinel mixed with alumina. Concentration of methane was suppressed below 1% even at 450 °C, while CO concentration gradually increased from 0.8%

to 3.1% when the temperature increased from 350 to 450 °C. The promotion effect of alumina suggests formation of methanol as an intermediate. However, methanol was scarcely detected in the product gas. Reaction rate of methanol steam reforming is much faster than that of dimethyl ether hydrolysis and the DME hydrolysis is considered as a rate-determining step in DME SR [16,18].

Although the spinel–alumina mixing ratio could affect the DME SR performance, the ratio was fixed at the spinel–alumina ratio of 2:1 in the present work. Tanaka et al. [16] reported the effect of the mixing ratio of Cu–Fe–Mn spinel and alumina on DME SR and the spinel–alumina mixing ratios of 1:1 and 2:1 were found to be the optimum ratios. The high alumina content (spinel:alumina = 1:8) gave a high DME hydrolysis activity, resulting in a high DME conversion at low temperatures below 350 °C. However, at higher temperatures, it exhibited low DME conversion since the amount of spinel is not sufficient enough to effectively proceed MeOH SR. The high spinel content (spinel:alumina = 8:1) led to low DME conversion because of insufficient amount of DME hydrolysis catalyst.

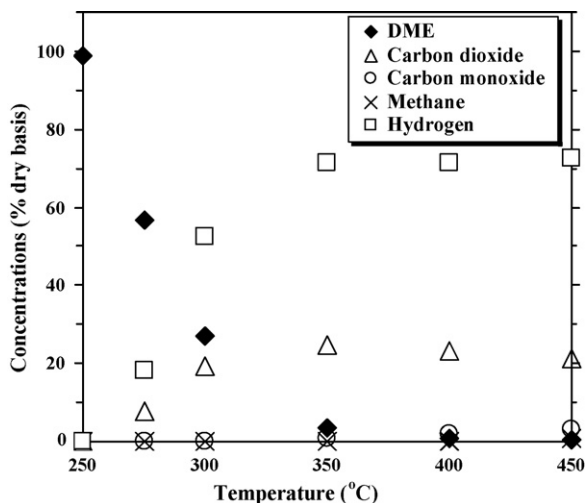


Fig. 11. Concentrations of DME and products of effluent reformat as a function of temperature from DME SR over Cu–Fe900 + ALO700. Reduction conditions: 350 °C, 3 h in 10% H<sub>2</sub>/N<sub>2</sub>. Reaction conditions: S/C = 2.5; DME = 16.7%, steam = 83.3%; GHSV = 4000 h<sup>-1</sup>.

#### 4. Conclusions

A composite catalyst of copper ferrite spinel (CuFe<sub>2</sub>O<sub>4</sub>) and alumina was highly active for dimethyl ether steam reforming (DME SR) for production of hydrogen. The influences of calcination temperatures of the copper spinel (500–1100 °C)

and that of alumina (500–1100 °C) were investigated. The crystallinity and reducibility of the copper ferrite spinel and the acidity of alumina were significantly influenced by the calcination temperature. The optimal calcination temperatures of  $\text{CuFe}_2\text{O}_4$  and alumina were at 900 °C, and at or below 700 °C, respectively. Gas hourly space velocity (GHSV), reforming temperatures, and mixing state played a role in DME SR. The composite catalysts both with and without pre-reduction were active for DME SR when the former exhibited higher initial activity. DME conversion (>95%) and hydrogen production rate ( $\sim 50 \text{ mol kg}_{\text{cat}}^{-1} \text{ h}^{-1}$ ) were achieved at  $T_r$  of 350 °C and GHSV of  $1500 \text{ h}^{-1}$ , when concentration of hydrogen and carbon monoxide were ca.73% and 2% on a dry basis without nitrogen dilution, respectively. In comparison to the commercial  $\text{CuFe}_2\text{O}_4$  mixed with  $\text{Al}_2\text{O}_3$  and  $\text{Cu/ZnO/Al}_2\text{O}_3$  mixed with  $\text{Al}_2\text{O}_3$ , the present composite catalyst of  $\text{CuFe}_2\text{O}_4$  and  $\text{Al}_2\text{O}_3$  markedly exhibited excellent activity for DME SR.

## References

- [1] T. Shishido, Y. Yamamoto, H. Morioka, K. Takaki, K. Takehira, *Appl. Catal. A: Gen.* 263 (2004) 249–253.
- [2] H. Oguchi, T. Nishiguchi, T. Matsumoto, H. Kanai, K. Utani, Y. Matsumura, S. Imamura, *Appl. Catal. A: Gen.* 281 (2005) 69–73.
- [3] J. Papavasiliou, G. Avgouropoulos, T. Ioannides, *Catal. Commun.* 6 (2005) 497–501.
- [4] E.S. Ranganathan, S.K. Bej, L.T. Thompson, *Appl. Catal. A: Gen.* 289 (2005) 153–162.
- [5] E.Y. Garcia, M.A. Laborde, *Int. J. Hydrogen Energy* 16 (1991) 307–312.
- [6] K. Vasudeva, N. Mitra, P. Umasankar, S.C. Dhingra, *Int. J. Hydrogen Energy* 21 (1996) 13–18.
- [7] F. Haga, T. Nakajima, H. Miya, S. Mishima, *Catal. Lett.* 48 (1997) 223.
- [8] F.J. Marino, E.G. Cerrella, S. Duhalde, M. Jobbagy, M.A. Laborde, *Int. J. Hydrogen Energy* 23 (1998) 1095–1101.
- [9] A. Heinzl, B. Vogel, P. Hubner, *J. Power Sources* 105 (2002) 202–207.
- [10] J.R.H. Ross, *Catal. Today* 100 (2005) 151–158.
- [11] R.J. Farrauto, *Appl. Catal. B: Environ.* 56 (2005) 3–7.
- [12] S.H.D. Lee, D.V. Applegate, S. Ahmed, S.G. Calderone, T.L. Harvey, *Int. J. Hydrogen Energy* 30 (2005) 829–842.
- [13] V.V. Galvita, G.L. Semin, V.D. Belyaev, T.M. Yurieva, V.A. Sobyenin, *Appl. Catal. A: Gen.* 216 (2001) 85–90.
- [14] K. Takeishi, H. Suzuki, *Appl. Catal. A: Gen.* 260 (2004) 111–117.
- [15] T. Matsumoto, T. Nishiguchi, H. Kanai, K. Utani, Y. Matsumura, S. Imamura, *Appl. Catal. A: Gen.* 276 (2004) 267–273.
- [16] Y. Tanaka, R. Kikuchi, T. Takeguchi, K. Eguchi, *Appl. Catal. B: Environ.* 57 (2005) 211–222.
- [17] T. Mathew, Y. Yamada, A. Ueda, H. Shioyama, T. Kobayashi, *Appl. Catal. A: Gen.* 286 (2005) 11–22.
- [18] K. Faungnawakij, Y. Tanaka, N. Shimoda, T. Fukunaga, S. Kawashima, R. Kikuchi, K. Eguchi, *Appl. Catal. A: Gen.* 304 (2006) 40–48.
- [19] J. Sato, N. Saito, Y. Yamada, K. Maeda, T. Takata, J.N. Kondo, M. Hara, H. Kobayashi, K. Domen, Y. Inoue, *J. Am. Chem. Soc.* 127 (2005) 4150–4151.
- [20] I. Cesar, A. Kay, J.A. Gonzalez Martinez, M. Gratzel, *J. Am. Chem. Soc.* 128 (2006) 4582–4583.
- [21] T.A. Semelsberger, R.L. Borup, *J. Power Sources* 152 (2005) 87–96.
- [22] K. Faungnawakij, R. Kikuchi, K. Eguchi, *J. Power Sources* 161 (2006) 87–94.
- [23] Y. Tanaka, T. Takeguchi, R. Kikuchi, K. Eguchi, *Appl. Catal. A: Gen.* 279 (2005) 59–66.
- [24] Y. Tanaka, T. Utaka, R. Kikuchi, T. Takeguchi, K. Sasaki, K. Eguchi, *J. Catal.* 215 (2003) 271–278.
- [25] P.S. Santos, H.S. Santos, S.P. Toledo, *Mater. Res.* 3 (2000) 104–114.